

Cladding Hoop Stresses in Spent PWR Fuel – Determination of Rod Internal Pressure as Initial Condition for Dry Storage

Albert J. Machiels

Electric Power Research Institute, Inc.
3420 Hillview Avenue
Palo Alto, CA 94304 USA
amachiel@epri.com

Joseph Y.R. Rashid

Anatech
5435 Oberlin Drive
San Diego, CA 92121
joe.rashid@anatech.com

Dion J. Sutherland

Anatech
5435 Oberlin Drive
San Diego, CA 92121
dion.sutherland@anatech.com

William F. Lyon

Anatech
5435 Oberlin Drive
San Diego, CA 92121
bill.lyon@anatech.com

ABSTRACT

The end-of-reactor-life (EOL) rod internal pressure (RIP) is the primary protagonist for several evolutionary changes during long-term dry storage that affect cladding resistance to failure when spent fuel assemblies are subjected to normal and accident conditions of transport. At the maximum temperature attained either during vacuum drying or dry storage, EOL RIP determines the maximum stress state in the fuel rod cladding, which in turn sets the initial conditions for potential time-dependent changes in the hydrides structure in the cladding as the latter undergoes slow cooling in the inert environment of the storage cask. An extensive literature search was conducted for pressurized water reactor (PWR) standard and Integral Fuel Burnable Absorber (IFBA) fuel to collect RIP and void volume data for the entire spent fuel population of Zircaloy-4, ZIRLO and M5 cladding designs. Only the non-proprietary data set was analyzed; no IFBA data were retained because only a small number of proprietary data points were identified. Use of bounding values for EOL RIP, would typically be of limited value, given that such values must be modified for the temperature and void volume distribution in the fuel rod that exists during vacuum drying or at the beginning of dry storage. Using the non-proprietary data set, a simple model was developed for calculating rod internal pressure, which can be derived from the universal gas law using rod gaseous contents (number of moles), void volume, and temperature profiles compatible with dry storage operations and conditions. Examples of calculations of initial stress cladding conditions for spent PWR fuel stored under vacuum inside a vertically positioned cask are provided taking advantage, in a simplified manner, on experimentally determined temperature profiles inside the storage system. For rod-average burnup of less than ~60 GWd/MTU, the examples show that initial cladding stress conditions are estimated to be less than 100 MPa for the vast majority of spent PWR fuel for which non-proprietary data are available.

1 INTRODUCTION

The end-of-life (EOL) rod internal pressure (RIP) is the primary protagonist for several evolutionary changes during long-term dry storage that affect cladding resistance to failure when spent fuel assemblies are subjected to normal and accident conditions of transport. At the maximum temperature attained either during vacuum drying or dry storage, EOL RIP determines the maximum stress state in the fuel rod cladding, which in turn sets the initial conditions for potential time-dependent changes in the hydrides structure in the cladding as the latter undergoes slow cooling in the inert environment of the storage cask. As time progresses, the cladding hydrides structure may change from a predominantly circumferential lamellar structure with radially varying concentration to a mixed circumferential and radial structure, the latter being highly undesirable because of its detrimental effect on the cladding ability to resist failure under pinch loading impact when cladding temperature drops below the cladding material's ductile-to-brittle transition temperature (DBTT). This behavior is highly dependent on the concentration and continuity of the radial hydrides structure [1], which is driven by the magnitude of RIP.

The results of a multi-year research effort to assess cladding performance under normal and hypothetical accident conditions of spent nuclear fuel transportation, summarized in EPRI-1015048 [2], indicate that cladding resistance to failure under the dynamic loading of some transportation accidents depends on fuel-cladding gap size and radial hydride formation, both of which evolve during long-term dry storage under the driving force of RIP. Consequently, knowledge of EOL RIP is of prime importance in assessing the performance of high burnup spent fuel during expected and hypothetical conditions of transport. However, RIP is highly dependent on fuel design and operational history, and cannot be characterized by a single quantity that represents the general behavior of spent fuel in the field. Furthermore, efforts undertaken in the above-cited research program to develop reliable estimates of EOL RIP have been curtailed by the paucity of available non-proprietary data. Rod internal pressure data at the start of dry storage, compiled from various sources at the time of the study, are contained in Figure 1.1 reproduced from Ref. 2.

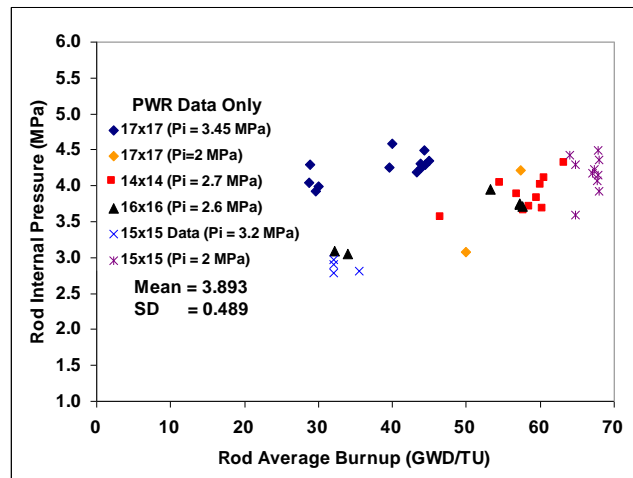


Figure 1.1. End of Life PWR Rod Internal Pressure at 25°C [2]

Although the data shown in Figure 1.1 were not extensive, they were, nevertheless, considered representative, but not necessarily sufficient to derive reliable estimates of conservative values for end-of-life rod pressures. Use of bounding values for EOL RIP, such as the system pressure licensing criterion, would typically be of limited value, given the desire to assess the actual performance of existing assemblies versus the theoretical performance of those assemblies. Even when bounding

values of EOL RIP can be determined from stylized reactor operating conditions, such values must be modified for the temperature and void volume distribution in the fuel rod that exists during vacuum drying or dry storage. For example, the measured temperature profiles in Figure 1.2 [3], which can be considered to be representative for high burnup (i.e., high heat load) fuel stored under vacuum within a vertically positioned cask, show axially varying temperature distribution with relatively lower plenum temperature. This temperature profile, when combined with axially varying void volume, would result in a different rod internal pressure than by directly applying the EOL RIP data scaled to the 400 °C temperature stipulated in the U.S. regulatory guidance. [4]

What is needed is to develop a model for combining spent fuel data, derived from measurements on several fuel designs having reached different burnup levels, from which rod internal pressure can be derived from the universal gas law using rod gaseous contents (number of moles), void volume, and temperature distributions compatible with dry storage operations and conditions. This is accomplished through the assessment described in this paper, which is the first in a series of studies intended to update the EPRI's multi-year study cited above.

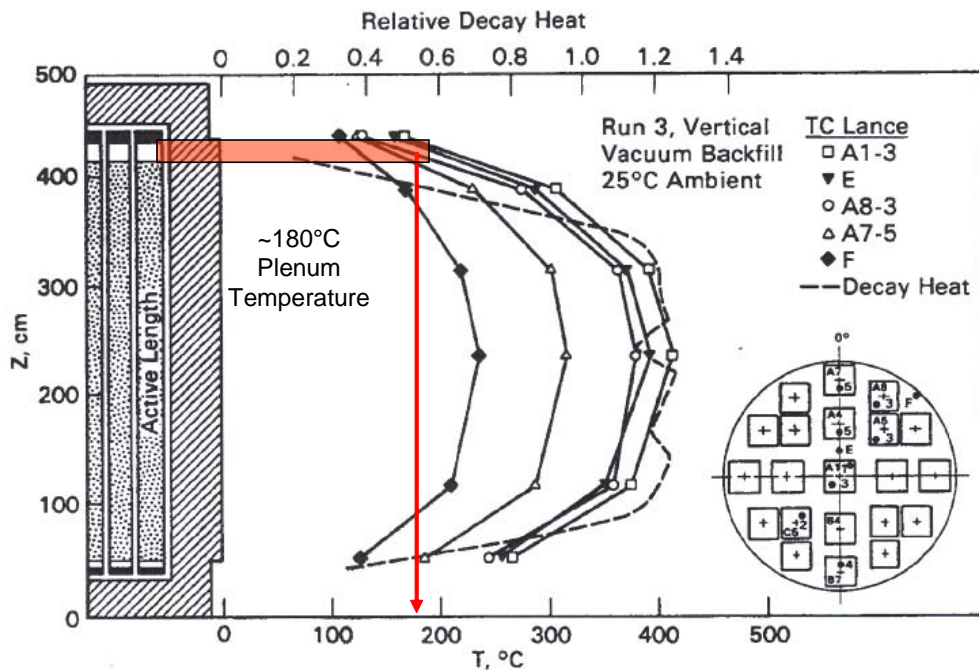


Figure 1.2. Axial Temperature Profiles for Vertical, Vacuum Test – EPRI NP-4887 [3]

The first step in this systematic assessment is to conduct a literature search to re-populate Figure 1.1 with available non-proprietary data, which when used in a newly developed extrapolation procedure, as discussed in this paper, can lead to the development of reliable estimates for the EOL RIP. The results of the literature search are given in Section 2. Section 3 describes the development of an extrapolation model and a basis for calculating the internal rod pressure as the initial condition for dry storage. For this purpose, the temperature-burnup basis of 25°C-60 GWd/MTU *rod-average* burnup has been chosen as the common basis for defining the rod internal pressure. Section 4 illustrates the procedure for calculating rod internal pressure in a dry storage cask using the model described in Section 3. Conclusions are presented in Section 5.

2 LITERATURE SEARCH FOR END-OF-LIFE ROD INTERNAL PRESSURE DATA

An extensive literature search was conducted for pressurized water reactor (PWR) standard and Integral Fuel Burnable Absorber (IFBA) fuel to collect RIP, void volume, and assembly-power distributions data for the entire spent fuel population of Zircaloy-4, ZIRLO and M5 cladding designs. Only the non-proprietary data set was analyzed; no IFBA data were retained because only three proprietary data points were identified. The EOL RIP data are summarized in Figure 2.1, and are subjected to a statistical analysis as described below.

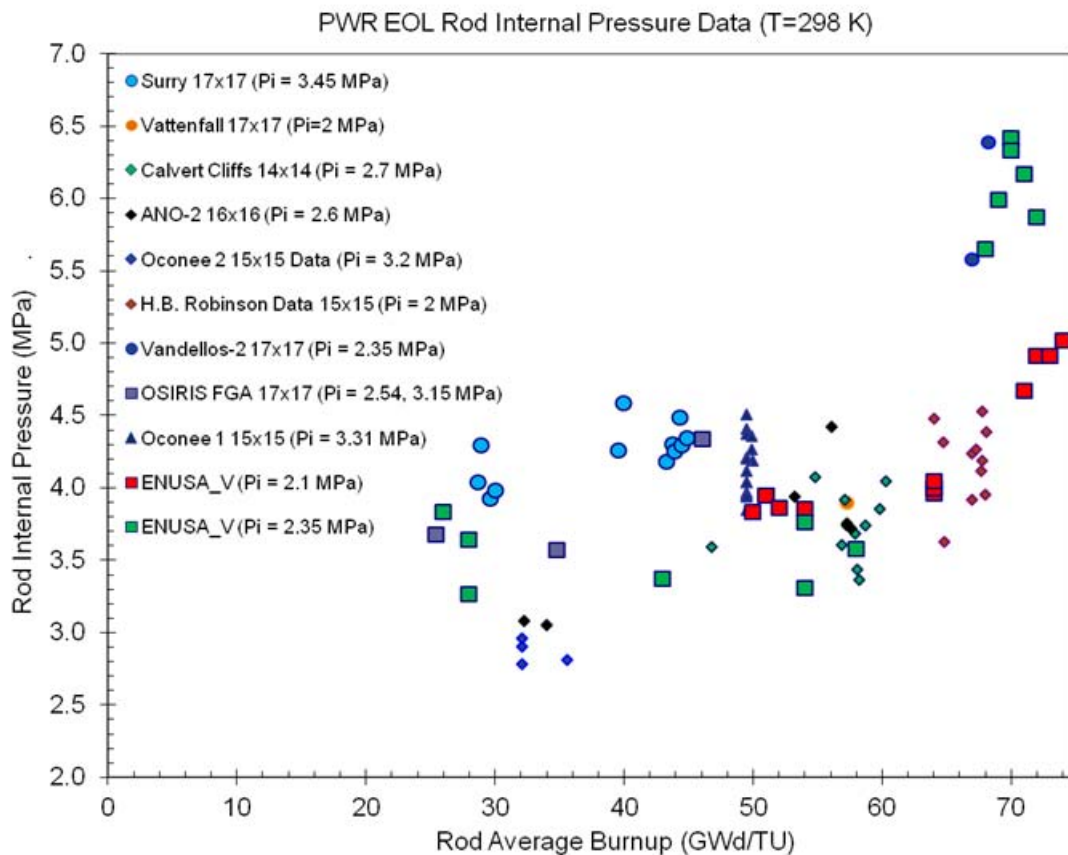


Figure 2.1. Rod Internal Pressure data for all fuel rod designs, (14x14, 15x15, 16x16, 17x17)

Examining the pressure-vs.-burnup trend in Figure 2.1 reveals that the EOL RIP begins to rise exponentially at a rod-average burnup level of ~ 60 GWd/MTU, which is close to the commercial fuel licensing limit of 62 GWd/MTU (rod-average burnup). A jump in EOL RIP values is noticeable at burnups higher than 68 GWd/MTU. This jump may be due to the fact that these rods are not truly representative, because they were originally not designed for such high burnups. The observed jump in internal pressures could result from the initial plenum volumes being too small to properly account for fuel swelling.

To avoid any statistical bias in the treatment of the data, only the EOL RIP for burnups up to 60 GWd/MTU are used in the statistical analysis, and RIP values for burnups above 60 GWd/MTU can be determined by extrapolation. Using this approach, the data in Figure 2.1 were subjected to regression analysis, and regression fits were developed for the best fit and \pm one standard deviation, as shown in Figure 2.2, which also shows the mean and standard deviation.

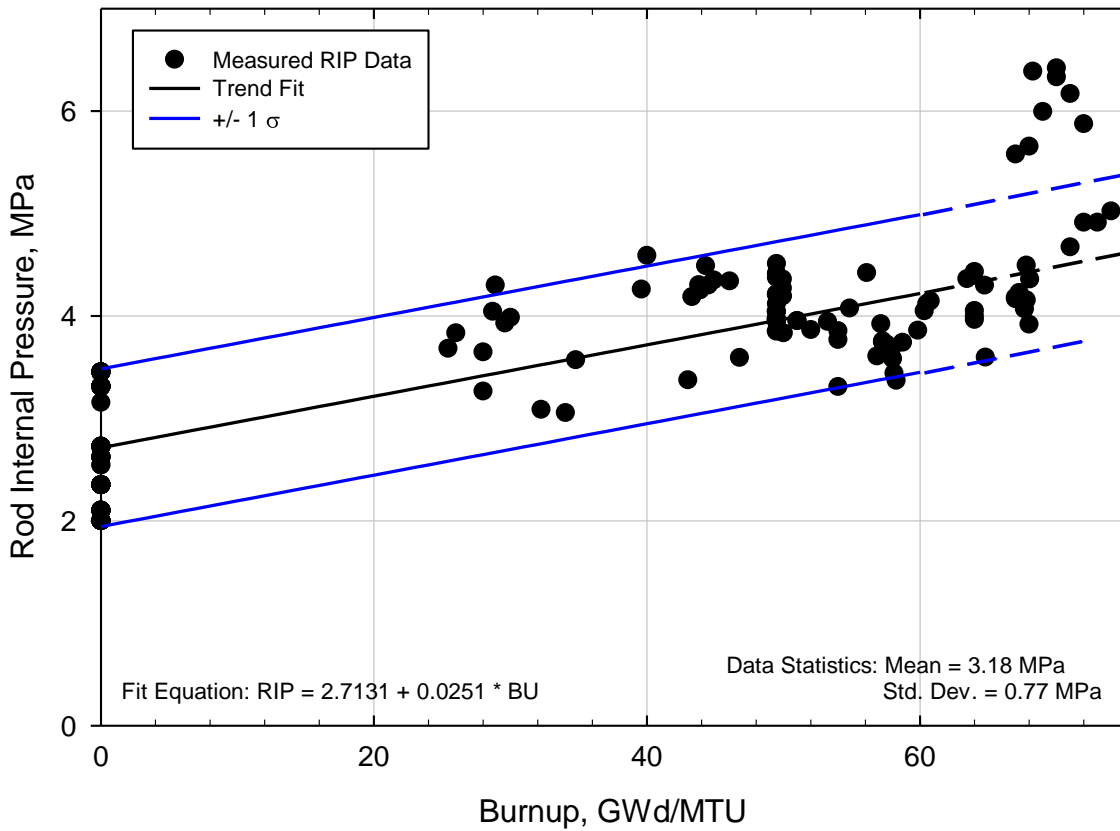


Figure 2.2 Statistical depictions of RIP Data for Burnups ≤ 60 GWd/MTU

The regression fit for the mean trend of the data in Figure 2.2 produces the following equation:

$$P = A + b * Bu , \quad (2.1)$$

where $A = 2.7131$, $b = 0.0251$, Bu stands for burnup in GWd/MTU.

The 1- σ regression fit is obtained simply by adding the 1- σ value (i.e., 0.77 MPa) to the ordinate.

3 PROCEDURE FOR CALCULATING ROD INTERNAL PRESSURE IN DRY STORAGE

3.1 Development of Extrapolation Model

In view of the fact that the current spent fuel inventory consists of many designs and fuel types, RIP becomes a non-unique descriptor of the amount of gas in a given fuel rod. Therefore, and to permit a generic treatment of the EOL RIP, the fuel rod gas content is quantified in terms of a single variable, namely, the number of moles of gas. Using the ideal gas law, and knowing the void volume and the temperature, one can determine the RIP as follows:

$$PV = nRT = NkT \quad (3.1)$$

where:

P is the pressure in Pascal

V is the volume in cubic meters

n = number of moles

R = universal gas constant = 8.3145 J/mol K

N = number of molecules

k = Boltzmann constant = 1.38066×10^{-23} J/K

$k = R/N_A$

N_A = Avogadro's number = 6.0221×10^{23} /mol

Equation 1 is inverted to give the number of gas moles, as follows:

$$n = PV / RT , \quad (3.2a)$$

for spatially uniform volume and temperature; and

$$n = (P/R) \sum_{i=1}^{i=4} (V_i / T_i) , \quad (3.2b)$$

for spatially varying volume and temperature.

Equation 3.2b is inverted to provide:

$$P = (nR) / \sum_{i=1}^{i=4} (V_i / T_i) \quad (3.2c)$$

The summation in Eq. 3.2b and 3.2c is taken over the four domains of the fuel rod void volume:

i=1 Upper plenum,

i=2 Lower plenum (in some rods)

i=3 Pellet-cladding gap

i=4 Pellet void volume, including pellet open porosity, cracks and dish volume

It is noted that domain 3, pellet-cladding gap, consists of axially varying volume and temperature, which require integration of the V_3/T_3 term over the axial length as shown in Equation 3.3:

$$V_3/T_3 = \int V(z)/T(z) dz = \sum_j 2\pi r G_j \Delta Z_j / ((T_F + T_C)_j / 2) \quad (3.3)$$

In the above equation, the summation is accomplished by dividing the fuel column into axial segments, where the subscript j stands for the j^{th} axial segment, r is the pellet radius, G is the fuel-cladding gap size, ΔZ is the axial segment height, and T_F and T_C are the fuel surface and cladding inner surface temperatures, respectively.

Similarly for domain 4, we have:

$$V_4/T_4 = \int V(z)/T(z) dz = \sum_j \pi r^2 v_j \Delta Z_j / T_{CL}, \quad (3.4)$$

where v is the fuel pellets open porosity, including pellet cracks and un-filled dish volumes and the small chamfer volumes, and T_{CL} is the fuel centerline temperature which, noting that the temperature is radially flat, represents pellet average temperature. Conservative estimates put the maximum value for v at less than 1%, based on general observations. This is equivalent to $\sim 20 \mu\text{m}$ for 17x17 design, and is assumed, for computational purposes, to be the minimum value that can exist although high-burnup fuel is expected to have zero fuel-cladding gap, if not actual bonding, over the central (high-power) portion of the fuel column.

For the practical implementation of Equations 3.3 and 3.4 for PWR high burnup rods for which typical fuel-cladding bonding exists, two idealized conditions could be considered: (1) Assuming no pellet-cladding gap over a large central portion of the rod, but with voids from cracks and other features present in the volume occupied by the pellets, i.e. $V_3 = 0$, but $V_4 \neq 0$; or (2) assuming a pseudo pellet-cladding gap along the length of the rod that would yield a void volume equivalent to that assumed for modeling option (1), i.e. $V_3 \neq 0$, but $V_4 = 0$. The choice between these two idealized conditions would not have a significant impact on internal pressure estimation, but would have a potentially important impact on cladding stress calculations: The pseudo-gap ($V_3 \neq 0$) assumption allows direct interactions between gas content and cladding, including the potential for rod volume increase due to thermal creep, while the no-gap ($V_3 = 0$) situation may result in greatly reduced cladding stress, but with attendant suppression of the potential for thermal creep. For practical purposes, internal pressure estimation being about the same for both situations, volume domains 3 and 4 can be treated as one. This means that, conservatively, Equation 3.3 would be used to treat both situations by increasing V_3 by a small amount to account for, without explicitly considering, V_4 . Based on the above mentioned estimate of v ($< 1\%$), this would be equivalent to using a residual gap size of $20 \mu\text{m}$, instead of zero, for high burnup fuel.

3.2 Conversion of EOL RIP to EOL Number of Moles

The EOL RIP data depicted in Figure 2.1, which was obtained by puncture measurements at 25°C , constitute a single volume/single temperature data. This makes Equation 3.2a the applicable equation. The input data for this equation is the pressure P , the void volume V and the temperature T , which was defined as 298K (25°C). Because not all the data points in Figure 2.1 have corresponding void volume measurements, the pressure data retained in this paper is a subset of the pressure data in Figure 2.1, and is depicted in Figure 3.1. The void volume data that matches the pressure data in Figure 3.1 is contained in Figure 3.2.

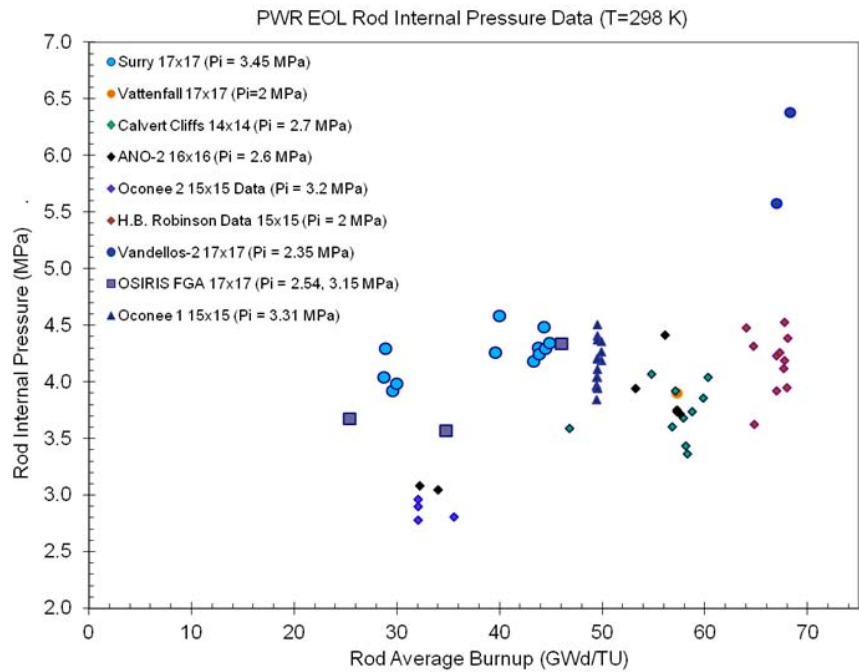


Figure 3.1. Rod Internal Pressure for all fuel rod designs, (14x14, 15x15, 16x16, 17x17), for which void volume data exists as shown in Figure 3.2

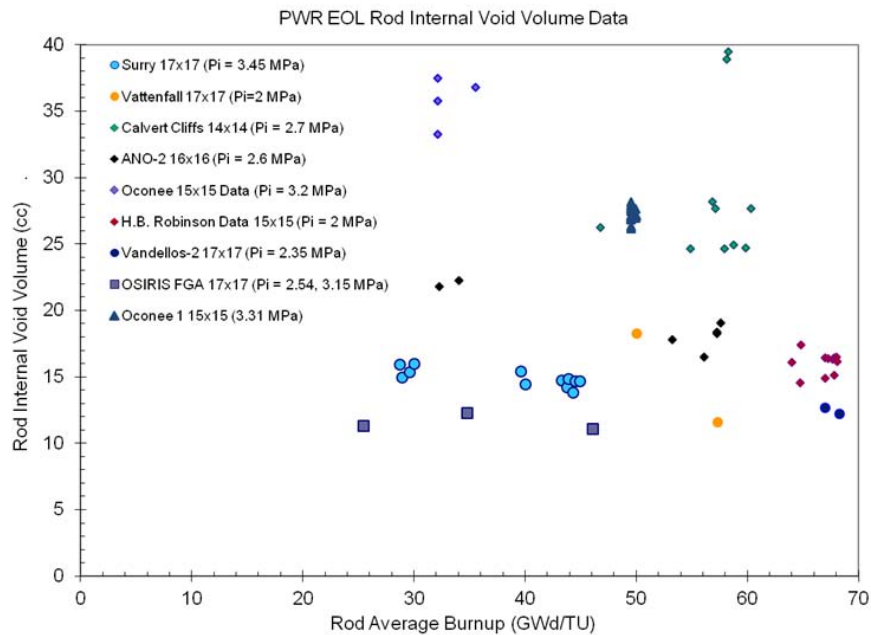


Figure 3.2. Void Volume for all fuel rod designs, (14x14, 15x15, 16x16, 17x17), for which pressure data exists as shown in Figure 3.1

Converting EOL RIP-versus-burnup data to moles-versus-burnup was accomplished by applying Equation 3.2a to each RIP point in Figure 3.1 with a corresponding volume value taken from Figure 3.2. The intent is to replace the pressure-burnup data by number-of-moles (n) versus burnup, as shown symbolically by Equation 3.5:

$$n = F(\text{Burnup}), \quad (3.5)$$

A graphical representation of Equation 3.5 is shown in Figure 3.3 for all available data, considering rods with burnup of 60 GWd/MTU or lower; the dashed lines in the figure signify extrapolation to higher burnup.

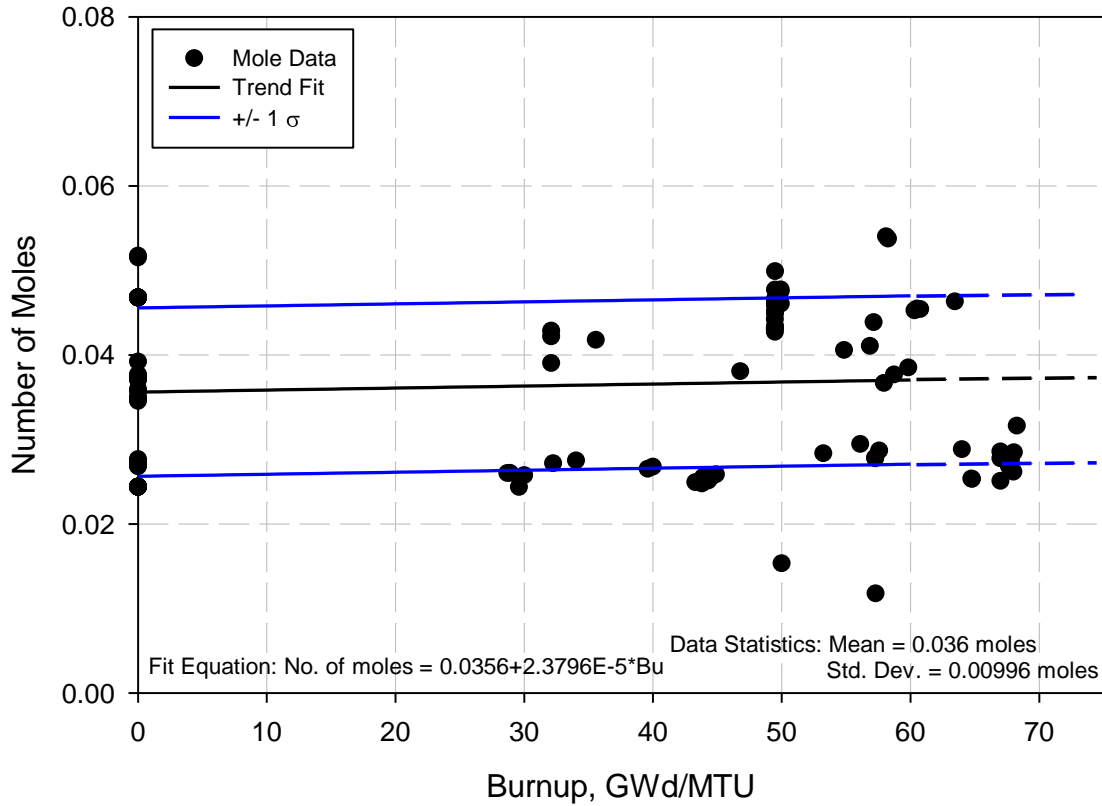


Figure 3.3. EOL Number of Moles as Function of Rod Average Burnup, inclusive of all available data

A regression fit for the trend of the data in Figure 3.3 produces the following equation:

$$n = A + b Bu, \quad (3.6)$$

where: $A = 0.0356$ and $b = 2.3795E-5$ for the mean values; as before, Bu stands for burnup in GWd/MTU.

It is interesting to note that it was fortuitous to limit the burnup to 60 GWd/MTU in Figure 3.3 because the trend shown in the figure for the number of moles versus burnup follows the same linear fit for the entire range of burnup. However, this was done to maintain consistency with Figure 2.2.

The fit for the number of moles in Figure 3.3 exhibits weak dependence on burnup, unlike the pressures data which show exponentially increasing dependence as burnup begins to rise above ~60 GWd/MTU. This weak dependence on burnup for rods below ~60 GWd/MTU may be attributed to the fact that the contributions of moles from fission gas release is generally small compared to the pre-pressurization inventory for the general population of fuel rods.

A graphical representation and statistical fits for the void volume are shown in Figure 3.4 for all available data, considering rods with burnup of 60 GWd/MTU or lower; the dashed lines in the figure signify extrapolation to higher burnup. Comparing Figure 3.4 to Figure 2.2 clearly shows the effect of the larger data scatter in the void volume compared to the internal pressure.

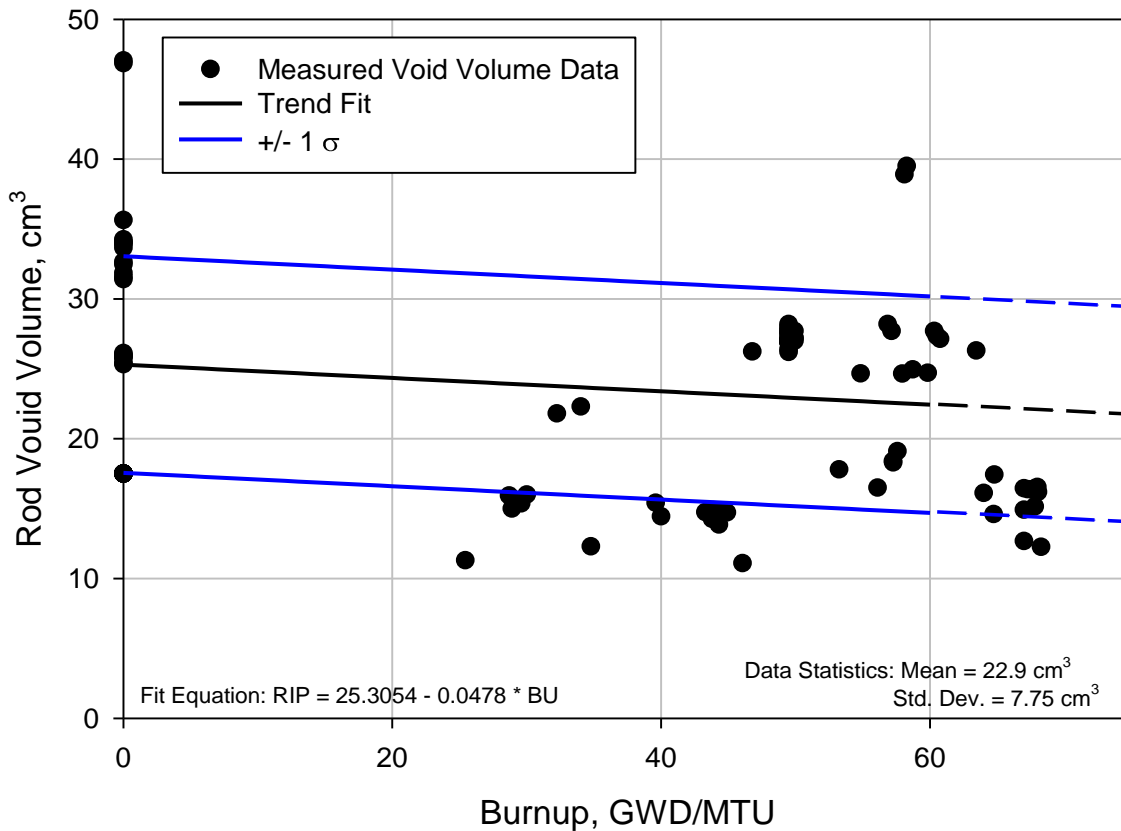


Figure 3.4. Statistical depictions of void volume data for burnup ≤ 60 GWd/MTU

A regression fit for the trend of the data in Figure 3.4 produces the following equation:

$$n = A + b Bu, \quad (3.7)$$

where: $A = 25.3054$ and $b = - 0.0478$ for the mean values; Bu stands for burnup in GWd/MTU.

4 EXAMPLES FOR CALCULATING CLADDING STRESS CONDITIONS FOR DRY-STORAGE APPLICATIONS

Application of the above set of equations to the calculation of rod internal pressure and resulting cladding stress in dry storage application is accomplished using the following steps:

1. Select the EOL rod-average burnup Bu
2. For the EOL rod-average burnup Bu , calculate the number of moles $n(Bu)$ from Equation 3.6
3. Construct a "virtual rod" that is representative of conditions of the rods in the dry storage system
4. Assume a temperature profile in the rod similar to Figure 1.2 with peak cladding temperature set at the chosen maximum temperature
5. Use the results of Step 4, calculate the rod internal pressure from equation 3.2c, extrapolated to the rod burnup, using the summation over the rods three volume domains, V_1 , V_2 and V_3 , noting that V_3 now includes V_4 :

$$P = n(Bu) * R / \sum_{i=1}^{i=3} (V_i / T_i) \quad (4.1)$$

The above approach is illustrated below, through hand calculations using Figure 1.2 temperature profile, and assuming a beginning-of-storage fuel-cladding residual gap to simulate pellets open porosity, namely V_4 ,

The calculations are performed for conditions assuming that thermal equilibrium conditions are established either during vacuum drying or at the beginning of dry storage.

1. Assume 60 GWd/MTU for Bu , and a 20- μm residual radial gap,
2. From Equation 3.6, $n = A + b Bu$ where,

$$A = 0.0356 \text{ and } b = 2.3796\text{E-}5 \text{ for the best-fit value,}$$

$$n = 0.037 \text{ moles,}$$

3. Virtual rod - Volume domains:

For the purpose of comparative evaluation, three void volumes are considered using Figure 3.4 to guide the choice of values: mean value at 60 GWd/MTU burnup, i.e., 22.4 cm³; mean value less 1σ , i.e., 14.7 cm³; and the lowest value in the data, i.e., ~12 cm³. These volumes are distributed in the two domains: upper plenum and the fuel-cladding gap volume, which has two temperature domains as shown in Figure 4.1. The fuel-cladding gap is assumed to be fixed at the minimum value of 20 μm , with a total volume for a 4-meter fuel column determined from the following formula:

$$V_3 = 2 \pi r G L = 2 * 3.14159 * 0.4 * 0.002 * 400 = 2.0 \text{ cm}^3$$

$$i=1 \text{ Upper plenum } V_1 = 20.4 \text{ cm}^3; 12.7 \text{ cm}^3; \text{ and } 9 \text{ cm}^3 \text{ as three void volume options}$$

$$i=2 \text{ Lower plenum} = 0$$

With reference to Figure 3.4, the three void volume options for V_1 are therefore chosen to correspond to the median void volume (22.4 cm^3), median less standard deviation (14.7 cm^3) and lowest data point value ($\sim 11 \text{ cm}^3$).

4. Temperature profile

$V_3 (= 2.0 \text{ cm}^3)$ is divided into three sub-volumes to correspond to the temperature profile shown in Figure 4.1 in green: a 2-meter long central region assumed to be at $400 \text{ }^\circ\text{C}$, and a 1-meter long (each) upper and lower region with an assumed linear temperature profile. The plenum temperature is assumed to be $180 \text{ }^\circ\text{C}$, as shown in the figure. From Fig. 4.1, the temperatures for $V_{3\text{-lower}}$ and $V_{3\text{-upper}}$ volumes are: $(180+400)/2 = 290 \text{ }^\circ\text{C}$.

$$V_{3\text{-lower}} = V_{3\text{-upper}} = 0.5 \text{ cm}^3 = 0.5\text{E-6 m}^3 \text{ each;}$$

$$V_{3\text{-center}} = 1.0\text{E-6 m}^3$$

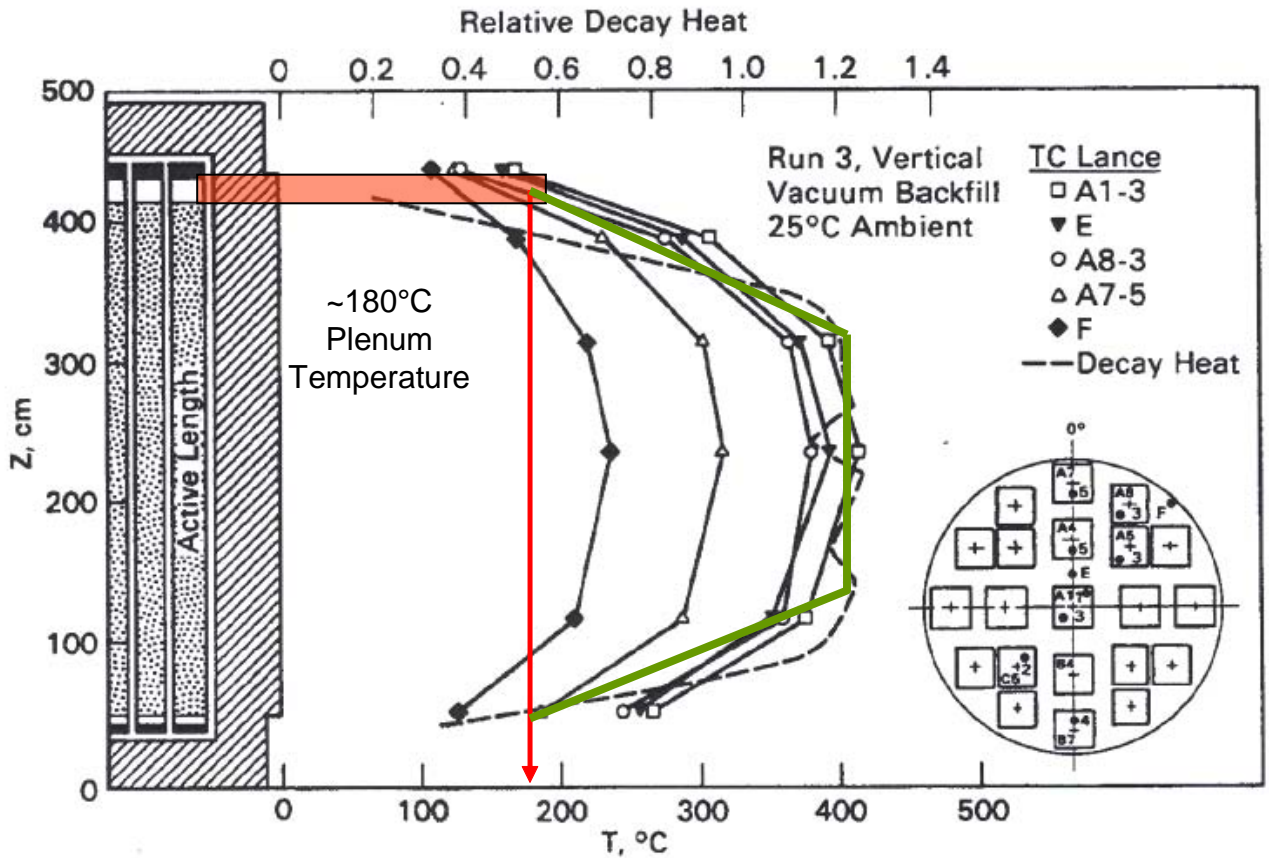


Figure 4.1. Axial Temperature Profiles for Vertical, Vacuum Test – EPRI NP-4887

5. Pressure and cladding stress calculations:

$$P = n(Bu) * R / \sum_{i=1}^{i=3} (V_i / T_i):$$

$$= 0.037 * 8.3145 / (20.4\text{E-6}/453 + 2 * 0.5\text{E-6}/563 + 1.0\text{E-6}/673) = 6.4 \text{ MPa.}$$

$$= 0.037 * 8.3145 / (12.7E-6/453 + 2 * 0.5E-6/563 + 1.0E-6/673) = 9.8 \text{ MPa.}$$

$$= 0.037 * 8.3145 / (9.0E-6/453 + 2 * 0.5E-6/563 + 1.0E-6/673) = 13.3 \text{ MPa.}$$

For a 17x17 fuel rod design: cladding thickness = 0.57 mm, outer diameter = 9.5 mm, inner diameter = 8.36 mm, and the mid-radius = $(9.5 - 2 * 0.57) / 2 = 4.18$ mm. The radius/thickness ratio = $4.18 / 0.57 = 7.33$. Assuming no fuel-cladding bonding that would likely reduce the load on the cladding wall, the mid-surface cladding hoop stress for nominal cladding thickness is:

$$\sigma_{\text{nom}} = 7.33 * P = 47, 72, 97 \text{ MPa for the three void volume options.}$$

A 90% effective cladding wall thickness (assuming ~100 μm of oxide thickness due to in-reactor waterside corrosion) raises the radius/thickness ratio to 8.26, which makes the mid-surface hoop stress:

$$\sigma_{\text{red}} = 8.26 * P = 53, 81, 109 \text{ MPa for the three void volume options.}$$

These pressure and stress values can be compared by simply using the EOL RIP data shown in Figure 2.2:

$$P = 2.7131 + 0.0251 * Bu = 4.219, \text{ for } Bu = 60 \text{ GWd/MTU}$$

Assuming a uniform temperature of 400 °C yields:

$$P = 4.219 * 673 / 298 = 9.53 \text{ MPa,}$$

and cladding hoop stress of:

$$\sigma_{\text{nom}} = 9.53 * 7.33 = 70 \text{ MPa for nominal thickness, and}$$

$$\sigma_{\text{red}} = 9.53 * 8.26 = 79 \text{ MPa for reduced cladding thickness}$$

Performing the same calculations when adding the standard deviation to the value of P at 25 °C (= 4.99 MPa) results cladding hoop stresses of 83 MPa and 93 MPa for the nominal and reduced cladding thickness.

These calculated pressure and stress conditions, however, only represent the initial conditions for the subsequent time-dependent evolutionary changes that will involve re-precipitation (possibly accompanied by reorientation) of the hydrogen in solid solution as a function of local cladding temperature, stress and hydrogen content.

During the very slow cooling process, cladding stress will be slowly reduced. Cladding stress may be further reduced to due cladding creep, which causes the fuel rod void volume to increase, assuming that fuel-cladding bonding is not sufficiently strong for impeding thermal creep. On the other hand, fuel-cladding bonding may be sufficiently strong such that cladding and fuel structurally form a composite material; in such a situation, cladding stresses are likely to be significantly lower than estimated when a gap between fuel and cladding is assumed to exist. After a period of time, local cladding temperatures reach levels where the hydrogen in solid solution begins to re-precipitate upon further cooling. This entire process has been previously investigated in the EPRI program, and will be further developed. This paper is therefore limited to the first step in the evaluation process.

5 CONCLUSIONS and OBSERVATIONS

End-of-life rod internal pressure data have been collected for fuel rod designs from available non-proprietary sources. By converting the pressure and void volume data to a single unique parameter, the subjective dependence of the pressure data on specific fuel rods design features was removed. This unique parameter, namely the number of moles of gas, allowed, through the use of the universal gas law, the derivation of a model for application to spent fuel in dry storage, for which temperature and void volume distributions differ significantly from in-reactor conditions.

An observation is that the trending for higher EOL RIP in the collected data for burnups in excess of the licensing limit of 62 GWd/MTU may not be due to burnup-dependent increase in fission-gas release, but rather due to the inability of fuel rods operating beyond their design limit to accommodate fuel swelling at higher burnup, given that rods, on which data were collected, were not initially designed for such high burnups. As a result, the paper restricts the treatment of the EOL RIP data for the model development to a rod-average burnup of ~60 GWd/MTU, which is of main interest to present spent fuel burnup levels.

Finally, the absence of IFBA fuel from the paper is due to the fact that no non-proprietary data is available. Based on the approach presented in this paper, IFBA fuel rods may very well fit in the existing data assuming design changes to accommodate the additional helium production.

6 REFERENCES

1. M.C. Billone, T.A. Burtseva, and R.E. Einziger, "Ductile-to-Brittle Transition Temperature for High-Burnup Cladding Alloys Exposed to Simulated Drying-Storage Conditions", *Journal of Nuclear Materials* 433 (2013) 431-448.
2. Spent Fuel Transportation Applications – Assessment of Cladding Performance, A Synthesis Report, EPRI Technical Report 1015048, December 2007.
3. The CASTOR-V/21 Spent-fuel Storage Cask: Testing and Analyses, Report NP-4887 (November 1986).
4. Spent Fuel Project Office Interim Staff Guidance - 11, Rev. 3, "Cladding Considerations for the Transportation and Storage of Spent Fuel," U.S. Nuclear Regulatory Commission (November 2003)
5. Fuel Analysis and Licensing Code: FALCON MOD01, Volume 1: Theoretical and Numerical Bases, EPRI Report 1011307, December 2004